Mendeleev Communications

Mendeleev Commun., 2027, **37**, in press

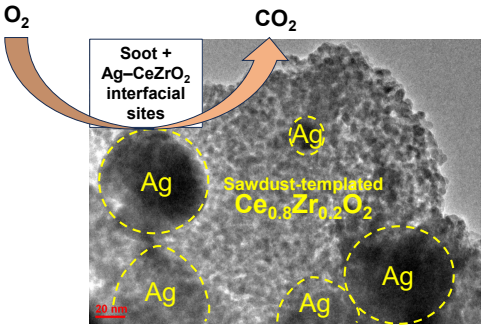
Effect of silver or potassium modification on sawdust-templated $Ce_{0.8}Zr_{0.2}O_2$ catalysts for soot oxidation

Igor Yu. Kaplin,*[a] Svetlana V. Bataeva,[a] Ekaterina S. Lokteva,[a] Oksana Ya. Isaikina[a] and Elena V. Golubina[a]

[a] *Department of Chemistry, M. V. Lomonosov Moscow State University, 119991 Moscow, Russian Federation. Fax: +7 495 939 4575; e-mail: kaplinigormsu@gmail.com*

DOI: 10.71267/mencom.8138

Sawdust-templated $Ce_{0.8}Zr_{0.2}O_2$ catalysts modified with Ag, KNO_3, and K_2CO_3 were studied in soot oxidation under tight-contact conditions. The silver-modified catalyst was more efficient than $Ce_{0.8}Zr_{0.2}O_2$ at low and medium temperatures, and the K_2CO_3-modified one, only at low temperatures; both potassium salts caused side reactions along with the combustion of soot and significant modification of the porous structure of $Ce_{0.8}Zr_{0.2}O_2$. The effectiveness of chemical modifiers was determined by the effect on redox properties provided that the optimal texture of the original mixed oxide was maintained, which ensured contact between the soot and the catalyst.



Keywords: ceria–zirconia, biomorphic catalyst, sawdust template, soot oxidation, silver, potassium nitrate, potassium carbonate.

Particulate filters are among the most effective technologies for reducing soot emissions from diesel engines. However, continuous soot accumulation gradually blocks the filter and necessitates its regeneration. A promising regeneration strategy is the use of catalysts capable of lowering the soot oxidation temperature to the range typical of diesel exhaust under operating conditions.[1–3] Ceria-based oxides are widely studied catalysts for soot oxidation owing to their high oxygen storage capacity, facile Ce^{4+}/Ce^{3+} redox cycling, and ability to form reactive oxygen species.[2–6] The incorporation of zirconium into CeO_2 improves the thermal stability and oxygen mobility of the fluorite lattice, while template synthesis allows for adjustment of the catalyst texture to improve contact with soot particles.[3–6] Previously, wood sawdust was used as an efficient biotemplate for the preparation of porous ceria-based materials.[7,8] The biomorphic route is attractive because it uses cheap renewable organic waste and gives oxide particles with a hierarchical texture inherited from wood.

The catalytic activity of the cerium–zirconium oxide in soot oxidation can be further tuned by chemical modifiers.[5,8] Silver is known to promote low-temperature oxidation reactions over ceria-based systems by facilitating oxygen activation and metal–support redox interactions.[9,10] Alkali metal compounds, especially potassium salts, are also considered as soot oxidation promoters due to their mobility, basicity, and ability to improve contact between soot and catalysts.[11–13] However, the effect of such modifiers on biomorphic oxides is poorly understood, and it is not necessarily positive as impregnation and repeated calcination can reduce the available surface area and clog pores. In this communication, we compare the effects of $AgNO_3$, KNO_3, and K_2CO_3 modification on the texture, phase composition, reducibility, and catalytic performance of wood sawdust-templated $Ce_{0.8}Zr_{0.2}O_2$ in soot oxidation.

The biomorphic $Ce_{0.8}Zr_{0.2}O_2$ catalyst (CZ) was prepared using pine sawdust as a template (the catalyst precursors and preparation procedures are provided in Online Supplementary Materials, Section S1). The target Ag content was 5 wt%, and potassium salt concentrations were 7 wt%. The samples were characterized by N_2 adsorption–desorption, X-ray diffraction (XRD) analysis, Raman spectroscopy, temperature-programmed reduction by H_2 (H_2-TPR), transmission electron microscopy with energy-dispersive X-ray analysis (TEM–EDX), and simultaneous thermal analysis coupled with mass spectrometry (STA–MS). Catalytic tests were carried out in air using a soot/catalyst mixture with a weight ratio of 1 : 20 under tight-contact conditions. The TG signal was used to calculate the apparent soot conversion as a function of temperature, while the MS signals were used to identify gaseous products evolved during heating. The characteristic temperatures T_{20}, T_{50}, and T_{90} were determined from the resulting $X(T)$ curves, and T_{max} was taken as the maximum temperature of the weight-loss rate in the corresponding DTG profile (see Online Supplementary Materials, Section S1).

According to XRD data (Section S2, Figure S1), all modified samples retained the fluorite-type structure of $Ce_{0.8}Zr_{0.2}O_2$. The calculated average $Ce_{0.8}Zr_{0.2}O_2$ crystallite size was 5–6 nm for all samples. No diffraction peaks due to Ag, KNO_3, K_2CO_3, or other crystalline phases including the atoms of modifiers were detected, suggesting either high dispersion of the modifiers or their presence in an X-ray amorphous state. Therefore, modifiers did not affect the crystal structure of CZ, but they changed its texture. Modification of CZ with silver and potassium salts resulted in a significant reduction in the BET surface area, while having only a minor effect on the total pore volume (Table 1). Thus, the wet impregnation and subsequent calcination partially destroyed or blocked the porous structure of the biomorphic oxide. The strongest textural deterioration was observed in the KNO_3-modified sample. The developed catalyst surface is very important for soot oxidation since this reaction is controlled not only by the intrinsic redox properties

© 2027 Mendeleev Communications

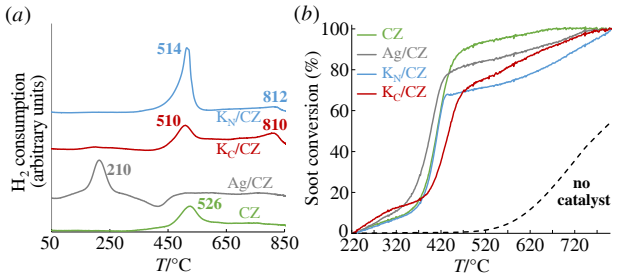


Figure 1 (*a*) H_2-TPR profiles of the catalysts; (*b*) soot conversion curves under tight-contact conditions in air. Heating rate, 10 K min^{-1}; soot/catalyst weight ratio, 1 : 20.

of the catalyst but also by the number of contact points between soot and the catalyst.

The Raman spectra (Section S2, Figure S2) confirmed the presence of potassium salts on the surface of the samples. In the spectrum of K_C/CZ, bands were observed at 1028 and 1060 cm^{-1}, which were attributed to vibrations of carbonate groups, while bands at 717 and 1050 cm^{-1} in the spectrum of K_N/CZ corresponded to nitrate groups. In contrast, the Ag modification did not cause the appearance of new bands in the Raman spectrum. A slight shift of the fluorite F_{2g} mode indicated a change in the local structure of CZ after impregnation with $AgNO_3$ and calcination.[9]

The H_2-TPR profiles [Figure 1(*a*)] revealed different effects of the modifiers on the reducibility of CZ. For K_C/CZ, broad peaks were observed at approximately 510 and 810 °C, as well as a weak peak at about 190 °C, likely related to the reduction of tightly bound surface carbonates. The K_N/CZ profile contained a very intense peak at 514 °C, which was attributed to thermal decomposition and reduction of nitrate species overlapping with the reduction of Ce^{4+} to Ce^{3+}.

For Ag/CZ, an additional low-temperature H_2 consumption peak appeared at about 210 °C. This signal can be interpreted taking into account both the thermal history of the sample and the possible partial oxidation of silver upon cooling in air. During calcination at 500 °C, $AgNO_3$-derived species decomposed to form bulk Ag_2O (>127 °C) and then Ag^0 (>230 °C).[14] However, when cooled in air, the surface of dispersed Ag particles can oxidize, especially at the Ag–$CeZrO_x$ interface. Therefore, the final Ag/CZ catalyst can contain metallic Ag together with surface $Ag^{\delta+}/AgO_x$ and interfacial Ag–O–Ce species.

The peak at about 210 °C corresponded to the absorption of 457 μmol of H_2 per gram. This value is too high to be explained solely by reduction of Ag_2O, assuming the target Ag loading of 5 wt %, because complete reduction of Ag_2O to Ag^0 would require only 232 μmol of H_2 per gram. Thus, the peak should be attributed to a superposition of several processes: the reduction of Ag_2O species, AgO_x-like species stabilized at the Ag–$CeZrO_x$ interface, and near-surface Ce^{4+} species, the reducibility of which increased upon contact with silver. The small negative signal can be related to the desorption of hydrogen species weakly adsorbed on metallic Ag or to a baseline effect of the TPR experiment. Significant H_2 dissolution in metallic silver or formation of a bulk silver hydride phase was unlikely since the Ag–H phase diagram showed very low hydrogen solubility in Ag.[15]

The catalytic data demonstrated that all catalysts greatly reduced the combustion temperature of soot [Figure 1(*b*)]. In the absence of a catalyst, soot oxidation started at 520 °C, whereas all catalysts provided a sharp increase in conversion already at 350–450 °C. For the CZ sample, T_{20}, T_{50}, T_{90}, and T_{max} were 380, 411, 471, and 411 °C, respectively (Section S3, Figure S3). Although K_C/CZ showed the highest activity in the low-conversion region below 320 °C, the modification with K_2CO_3 did not improve the main soot oxidation step: T_{20} and T_{50} increased. The STA–MS profile of K_C/CZ (Online Supplementary Materials, Section S3, Figure S4) contained a high weight-loss step in the range of 350–500 °C, accompanied by intense CO_2 evolution with a maximum of *m/z* 44 at 436.8 °C and a DTG minimum at 411 °C. Therefore, this temperature region can be assigned predominantly to catalytic soot oxidation. The low-temperature endothermic signals observed at about 100–150 °C were not related to soot combustion, and they can be attributed to desorption of water and weakly bound surface species.

Table 1 Textural and catalytic characteristics of the samples.

Sample	D^a/nm	$S_{BET}{}^b$/ $m^2\ g^{-1}$	$V_{BJH}{}^c$/ $cm^3\ g^{-1}$	$T_{20}{}^d$/°C	$T_{50}{}^d$/°C	$T_{90}{}^d$/°C	$T_{max}{}^e$/ °C
CZ	5 ± 1	60 ± 6	0.156	380	411	471	411
Ag/CZ	6 ± 1	23 ± 2	0.150	357	398	624	398
K_N/CZ	5 ± 1	6 ± 1	0.120	384	413	724	411
K_C/CZ	5 ± 1	33 ± 3	0.139	393	438	650	411

[a] The average CZ crystallite size calculated using the Scherrer equation. [b] The specific surface area calculated by the BET method. [c] The total pore volume calculated by the BJH method. [d] T_x are the temperatures corresponding to *x*% soot conversion. [e] The temperature of the maximum weight-loss rate, corresponding to the maximum soot oxidation rate.

The high-temperature part of the soot oxidation curve for K_C/CZ should be discussed separately from the main soot oxidation process. Potassium carbonate mainly occurs in γ- and β-polymorphic forms; the γ-K_2CO_3 phase is converted into β-K_2CO_3 at 421 °C, while the β-form melts at approximately 900°C.[12] Since K_C/CZ was calcined at 500 °C during synthesis, the presence of β-K_2CO_3 in the final sample was expected. Consequently, the weight loss observed after the main CO_2 evolution peak, especially at temperatures of 600–900 °C, can include slow transformations of carbonate species and, at higher temperatures, melting and partial decomposition of K_2CO_3 with the formation of K_2O and CO_2. These processes make a significant contribution to the shape of the kinetic curve in the high-temperature region.

A different behavior was observed for K_N/CZ. In the low- and medium-temperature ranges, its T_{20} and T_{50} values (384 and 413 °C, respectively) were close to those of CZ and noticeably lower than those of K_C/CZ. The STA–MS data (Section S3, Figure S5) confirmed that the main weight-loss step for K_N/CZ in the range of 350–470 °C was accompanied by intense CO_2 evolution with a maximum at 416 °C. However, in contrast to K_C/CZ, NO_x-related signals were observed in this case simultaneously: the *m/z* 30 signal increased in the same temperature range, and a weaker *m/z* 46 signal was observed near the exothermic peak of soot oxidation. This fact indicates that nitrate-containing species were not merely spectators during soot oxidation, but they could participate in the reaction, for example, through nitrate/nitrite transformations or NO_x-assisted oxidation pathways at the soot–catalyst interface.

The high-temperature part of the catalytic curve for K_N/CZ should be interpreted separately. The apparent T_{90} increased to 724 °C. It is well known that KNO_3 melts without decomposition at 530 °C.[12] Its decomposition begins at approximately 650 °C, yielding potassium nitrite, O_2, and trace amounts of NO_2. At around 800 °C, KNO_2 undergoes intense decomposition with the formation of N_2, O_2, and K_2O. Therefore, KNO_3 decomposition was not expected under the calcination conditions used for the synthesis of K_N/CZ. Consequently, nitrate species can remain in the catalyst and contribute to the TG signal during catalytic testing and non-isothermal STA–MS studies above 600 °C. This is consistent with the STA–MS data: an additional *m/z* 30 contribution was observed in the region around 700–900 °C, where no CO_2 evolution peak was present.

Among the modified samples, Ag/CZ provided the most significant improvement in catalytic properties in comparison with CZ at low and medium soot conversions: T_{20} and T_{50} decreased from 380 to 357 and from 411 to 398 °C, respectively. These changes indicate that Ag promoted low-temperature activation of oxygen and soot oxidation at sufficiently tight soot–catalyst contacts. However, at high soot conversions, Ag/CZ became less efficient than CZ. The most probable reason is the significantly lower surface area, which weakened the catalyst contact with soot particles after partial soot removal. The Ag/CZ catalyst was calcined at 500 °C after impregnation with $AgNO_3$. Consequently, the high-temperature part of the conversion curve should not be associated with the decomposition of residual silver nitrate. This conclusion was supported by the STA–MS data (Section S3, Figure S6): no signals corresponding to nitrogen oxides, which would be expected upon decomposition of residual nitrate species, were detected in the evolved gases. In addition, no distinct endothermic effects attributable to decomposition of silver-containing species were observed; the only broad endothermic signal was due to water desorption at 107°C.

The TEM–EDX data for Ag/CZ are presented in Section S4 (Figures S7 and S8). The catalyst contained relatively large Ag particles (20–250 nm), but the presence of highly dispersed Ag_2O particles, which can be difficult to detect by TEM, cannot be excluded.

The modification of soot combustion by adding silver to $Ce_{0.8}Zr_{0.2}O_2$ can be explained by the formation of dispersed Ag–$CeZrO_x$ interfacial sites that facilitated oxygen activation and its transfer to soot. At the same time, the high-temperature tail of the Ag/CZ conversion curve indicated that this redox promotion was efficient for soot particles in good contact with the catalyst, whereas the oxidation of poorly contacted soot remained delayed. Therefore, improving the dispersion of Ag and increasing the fraction of Ag–$CeZrO_x$ interface species can be a promising way to enhance the catalytic performance of biomorphic CZ-based catalysts. Potassium salts undergo high-temperature transformations, including nitrate/nitrite processes for K_N/CZ and carbonate-related processes for K_C/CZ, which can disturb soot–catalyst contacts and do not improve activity relative to CZ.

Thus, the catalytic performance of sawdust-templated ceria–zirconia catalysts cannot be rationalized only by changes in BET surface areas. The decisive factors are the nature of the modifier, its thermal stability, its ability to create redox-active interfacial sites or salt-derived reaction pathways, and the preservation of effective soot–catalyst contacts within the biomorphic pore system. These results show that chemical modification of biomorphic $CeZrO_x$ oxides is beneficial only when no significant texture deterioration is observed, and redox promotion is achieved without introducing high-temperature side processes that distort or limit soot oxidation.

This work was carried out in accordance with state assignment no. AAAA-A21-121011990019-4.

Online Supplementary Materials

Supplementary data associated with this article can be found in the online version at doi: 10.71267/mencom.8138.

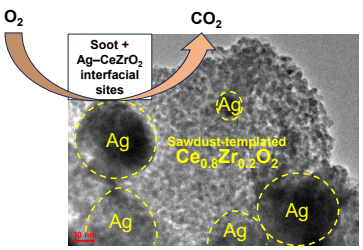
References

1 A. Yu. Stakheev, A. M. Gololobov, G. N. Baeva, G. O. Bragina and N. S. Telegina, *Mendeleev Commun.*, 2010, **20**, 269; https://doi.org/10.1016/j.mencom.2010.09.009.
2 T. Montini, M. Melchionna, M. Monai and P. Fornasiero, *Chem. Rev.*, 2016, **116**, 5987; https://doi.org/10.1021/acs.chemrev.5b00603.
3 Z. Tu, G. Wu, C. Zheng, X. Wu, J. Wan and S. Liu, *J. Rare Earths*, 2025, **43**, 641; https://doi.org/10.1016/j.jre.2024.08.017.
4 E. Sartoretti, F. P. Hagen, C. Novara, M. Piumetti, H. Bockhorn, D. Trimis and S. Bensaid, *J. Environ. Chem. Eng.*, 2026, **14**, 123057; https://doi.org/10.1016/j.jece.2026.123057.
5 A. Bueno-López, *Appl. Catal., B*, 2014, **146**, 1; https://doi.org/10.1016/j.apcatb.2013.02.033.
6 D. Fino, S. Bensaid, M. Piumetti and N. Russo, *Appl. Catal., A*, 2016, **509**, 75; https://doi.org/10.1016/j.apcata.2015.10.016.
7 I. Yu. Kaplin, E. S. Lokteva, E. V. Golubina, K. I. Maslakov, N. E. Strokova, S. A. Chernyak and V. V. Lunin, *RSC Adv.*, 2017, **7**, 51359; https://doi.org/10.1039/C7RA10791A.
8 I. Yu. Kaplin, E. S. Lokteva, S. V. Bataeva, K. I. Maslakov, A. V. Fionov, A. V. Shumyantsev, O. Ya. Isaikina, A. O. Kamaev and E. V. Golubina, *Pure Appl. Chem.*, 2021, **93**, 447; https://doi.org/10.1515/pac-2020-1012.
9 M. V. Grabchenko, N. N. Mikheeva, G. V. Mamontov, M. A. Salaev, L. F. Liotta and O. V. Vodyankina, *Catalysts*, 2018, **8**, 285; https://doi.org/10.3390/catal8070285.
10 H. Wang, S. Luo, M. Zhang, W. Liu, X. Wu and S. Liu, *J. Catal.*, 2018, **368**, 365; https://doi.org/10.1016/j.jcat.2018.10.018.
11 S. Liu, X. Wu, D. Weng and R. Ran, *J. Rare Earths*, 2015, **33**, 567; https://doi.org/10.1016/S1002-0721(14)60457-9.
12 M. S. Gross, M. A. Ulla and C. A. Querini, *Appl. Catal., A*, 2009, **360**, 81; https://doi.org/10.1016/j.apcata.2009.03.011.
13 W. Shan, L. Yang, N. Ma and J. Yang, *Chin. J. Catal.*, 2012, **33**, 970; https://doi.org/10.1016/S1872-2067(11)60385-9.
14 K. H. Stern, *J. Phys. Chem. Ref. Data*, 1972, **1**, 747; https://doi.org/10.1063/1.3253104.
15 P. R. Subramanian, *J. Phase Equilib.*, 1991, **12**, 649; https://doi.org/10.1007/BF02645164.

Received: 6th July 2026; Com. 26/8138

Contents entry

Effect of silver or potassium modification on sawdust-templated $Ce_{0.8}Zr_{0.2}O_2$ catalysts for soot oxidation



Igor Yu. Kaplin, Svetlana V. Bataeva, Ekaterina S. Lokteva, Oksana Ya. Isaikina, Elena V. Golubina